sciendo
Strojnícky časopis – *Journal of* MECHANICAL ENGINEERING,
VOL 74 (2024), NO 3, 27 - 44
STU SjF

WAY OF STRESS AND DEFORMATION CALCULATIONS IN THE RAILS AND ANCHOR PINS OF MINING RACK-RAILWAY TRACK

FRYDRÝŠEK Karel [1*,2], FREIS Jiří [3], KOLÁŘ Václav [4]

[1] *Faculty of Mechanical Engineering, VSB – Technical University of Ostrava, Department of Applied Mechanics, 17. listopadu 2172/15; 708 00 Ostrava, Czech Republic; karel.frydrysek@vsb.cz*
[2] *Faculty of Medicine, University of Ostrava, Institute of Emergency Medicine, Syllabova 19, 703 00 Os-trava-Vítkovice, Czech Republic*
[3] *Faculty of Mechanical Engineering, VSB – Technical University of Ostrava, Department of Machine and Industrial Design, 17. listopadu 2172/15; 708 00 Ostrava, Czech Republic*
[4] *Faculty of Electrical Engineering and Computer Science, VSB – Technical University of Ostrava, Department of Electrical Engineering, 17. listopadu 2172/15; 708 00 Ostrava, Czech Republic*

Abstract: Article deals with the calculation issues of deflection and stress in the rail and pins, which are a part of the anchoring design for rack-railway tracks. The rack-railway track, is intended for the transport of excessively heavy loads and people inside mines. A longitudinal track dip can be up to ± 35deg. Practical application is focused on the calculations of pins and rails, for which a novel combination of analytical approaches and FEM is used, with dynamic loading and the theory of beams on an elastic foundation. The methodology is explained in details and the first results are listed. Everything stated in this article can be used to design transport systems not only in mining/underground constructions.

KEYWORDS: rack-railway track, anchor pins, mining, stress, deformations, analytical approach, numerical approach, elastic foundation

1 Introduction

A rack-railway (also a rack-and-pinion railway or cog-railway) is a steep grade rail-way with a toothed rack rail, usually between the running rails. The first rack-railway was the Middleton Railway between Middleton and Leeds in West Yorkshire in England, UK, in the year 1812. Between the years 1903 and 1909, the McKell Coal and Coke Com-pany in Raleigh County in West Virginia installed a 35000 feet (i.e. 10700 m) long Morgan rack-rail track in its mines. Finally, a large number of different rack systems have been developed. Today, the most popular of rack-railways use the Abt system.

Good rail-track standards are fundamental for the safe and efficient operation of rail transport systems underground in mines. The design and layout of a rail track needs to be incorporated into the overall planning of the mine to ensure that practical payloads and an acceptable transport times are achievable. In particular, mine roadways should be de-signed to have adequate clearances, suitable gradients and the largest practical radii on curves. A careful selection of rail-track components, the use of competent tracklayers, and installing a track to a suitable specification etc. will enhance safety and significantly re-duce future maintenance needs.

For more information about rack-railways, see references [1–4].

The rack-railway track (manufacturer Ferrit , see Fig. 1 and references [1], [4] and [5], is in-tended for the transport of heavy loads in mines (an environment with a potentially ex-plosive atmosphere, containing methane and coal dust). The loads are transported by underground

DOI: 10.2478/scjme-2024-0031, Print ISSN 0039-2472, On-line ISSN 2450-5471

track, see Fig. 2(a), consisting of sections, see Fig. 2(b). In the middle of each section a toothed rack is welded, transmitting the peripheral forces of a lantern wheel in the electrohydraulic truck of a mining train (i.e. transfer cars) onto a track. The maximum longitudinal grade with an electric traction mean is ± 35deg and the maximum longitudinal grade with a rack-railway diesel locomotive is ± 25deg. The maximum lateral grade of the track is ± 10deg. The wheelbase for rails is 600/900 mm.

(a)

(b)

Fig. 1 Rack-railway track (a) Whole system, see [6], (b) Detail – an example of a train unit

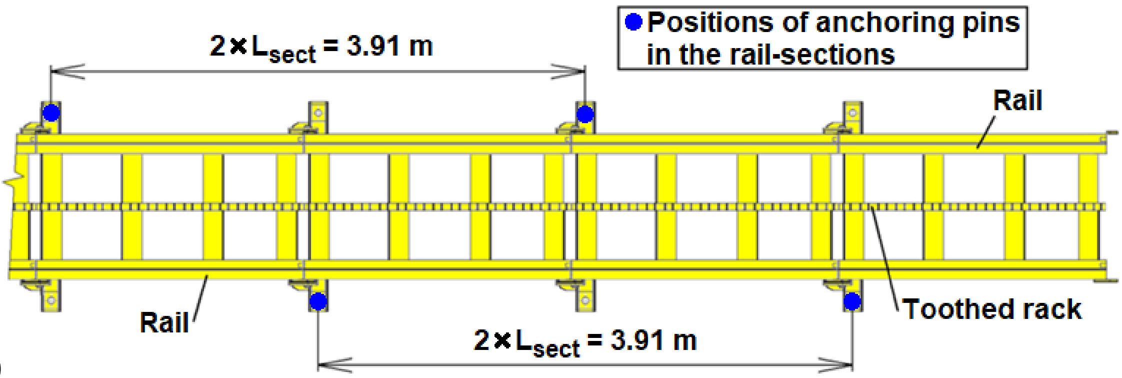

(a)

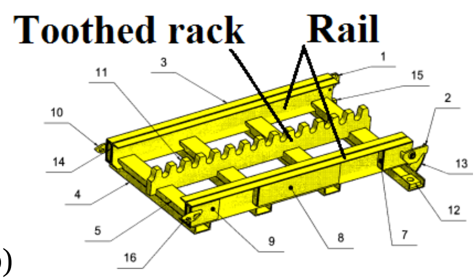

(b)

Fig. 2 (a) System of joined sections of a rack-railway track placed on a footwall (ground plan) and (b) the perspective projection and design of one section

A rack-railway track (i.e. the system of sections placed on a footwall) is secured by anchor pins with D_S /m/ diameter, see Fig. 2 and 3. These pins are inserted into the footwall (in turns on both sides of these sections) using pre-drilled holes filled with an adhesive. After this adhesive hardens sufficiently rigid and reliable mounts for rail tracks are formed.

The following text pays attention to the calculation of stresses and deflections in the rail sections and to the anchor pins for mining tracks (i.e. mechanics). Calculations, car-ried out depending on the angle of track inclination, shall be valid for the theory of beams on an elastic Winkler foundation. An original analytical solution is used in accordance with the theory of the 2nd order in mechanics combined with the Finite Element Method (FEM) solution, according to the theory of the easier 1st order in mechanics. Theory of 2nd order and its advantages are explained and applied in [7,8].

However, there is not enough information about stresses and deflections in the min-ing rail sections and their anchor pins, see [6,9–12]. There were not find the exact refer-ences about the keywords “mining”, “rack-railway track” “anchoring”, “stress, strain or deformation” and “calculation/solution”. From this reason, the authors wrote this article.

Load in our solved problem is defined by an emergency (extreme) situation that is linked to the sudden braking in stopping the train (the so-called hard stop). The results can be used as a method to design rails, pins and section mountings in the mines or other types of rail roads.

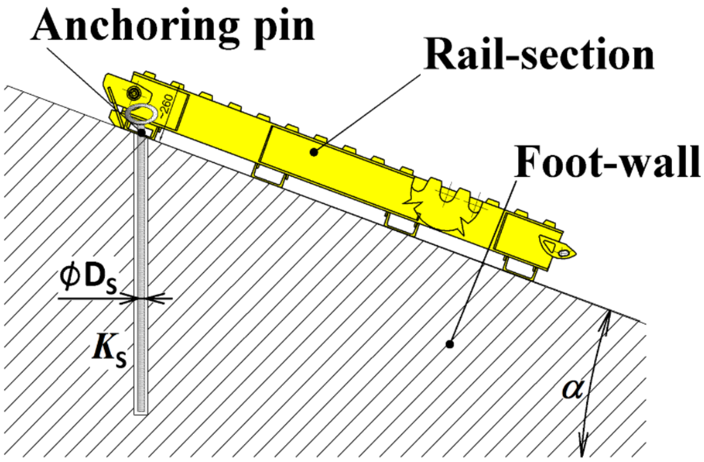

Fig. 3 One rail-section (section) placed on a footwall and secured by anchor pins

For an explanation of the 1st order theory in solid mechanics, it is a simpler and common approach for most engineering problems in mechanics, because the force and momentum equilibrium of a solid is analysed using a non-deformed system.

The theory of the 2nd order addresses a solid body equilibrium using a deformed sys-tem (i.e. the influence of the load usually changes the dimensions of such a solid, includ-ing the distribution of forces, their operation and moment effects). The advantage of the 2nd order theory is its greater accuracy, but the disadvantage is a more complex solution, as the configurations of the deformed system are also unknown. Because the more precise relations in the theory of the 2nd order are already derived for pins, it is useful to use them, see the following Chapter 2 (Tab. 1 to 3). Generally, the best-known application of the 2nd order theory are problems based on the Euler method for the buckling (i.e. stability) of beams.

First basic information presented in article was published in [6]. However, the ownership of copyright of [6] remains with the decision of main authors of this article and therefore a few pictures and tables were “reused” with small modification and with ap-propriate citation.

2 The anchor pin as a beam on an elastic foundation (deformations and loads)

Based on the design of the sections placement under the angle α /deg/, see Fig. 3 and 4, we can envision an anchor pin with a diameter D_S as a semi-infinite beam partially placed on the elastic (bilateral Winkler) foundation and loaded with general force F /N/ (including the horizontal force $F_1 = F\cos\alpha$ /N/ and vertical force $F_2 = F\sin\alpha$ /N/).

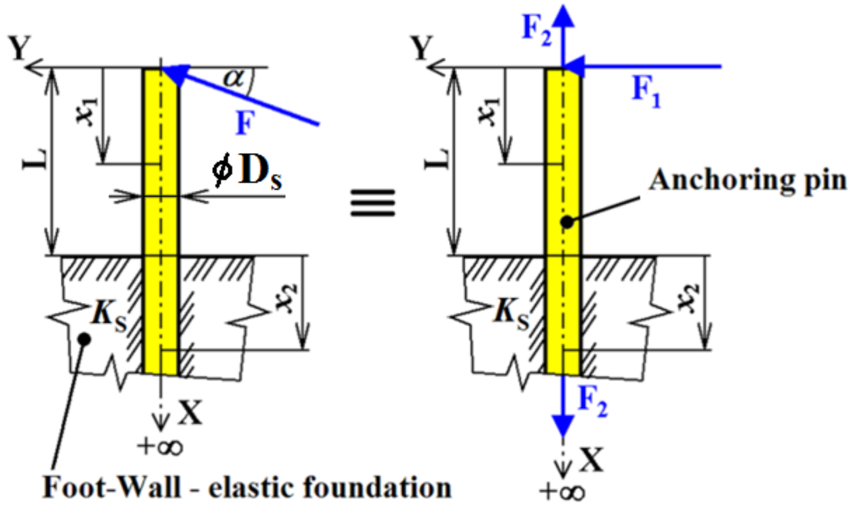

Fig. 4 A pin as a semi-infinite beam partially placed on an elastic foundation (a) External loading of a beam, (b) Loading by forces F_1 and F_2

The forces F_1 and F_2 result from interactions with rails sections, on which the dynamic load acts from the fully loaded and braking train (the hard stop). An analysis of the dynamic load is given in Chapter 3. The specific values of F_1 and F_2 are determined from the results of FEM calculations, see Chapters 4 and 5 of this article.

More information on the elastic foundation can be found in the literature [5,13-20]. Semi-infinite beams, as well as the infinite beams on elastic foundations, usually well represent the replacement of real long beams (i.e. the error of the model calculation is negligible). A semi-infinite beam, as a suitable approximation of a pin, thus provides a simple and fast solution with a minimal error.

For stiffness of the anchor pin subsoil, k_S /Pa/ applies according to Winkler $k_S = K_S D_S$, where K_S /Nm^{-3}/ is a module of the subsoil (material parameter), see Fig. 3 and 4.

In the following subchapters, there are important analytical solutions for intervals $x_1 \in (0;\ L)$ and $x_2 \in (0;\ \infty)$, i.e. the application of a beam of semi-infinite length partially supported by an elastic foundation and loaded via combination of compression and bending or tension and bending.

2.1 Loading by combination of compression and bending

In accordance with the knowledge, experience and results from the literature [5,13–16], from the theory of the 2nd order we can derive general relations for the horizontal deflection of the pin v /m/ and relations for slope $\frac{dv}{dx}$ /rad/, bending moment M_o /Nm/, shearing force T /N/ and the normal force N /N/, see Tab. 1 and 2. These relationships apply in local coordinate systems $x = x_1 \in (0;\ L)$ m and $x = x_2 \in (0;\ \infty)$ m, defined in Fig. 4 and Tab. 1 and 2. It is clear that the section x_1 is free of any subsoils (i.e. without an elastic foundation) and that section x_2 is surrounded by an elastic foundation (i.e. surrounded by foot-wall), L /m/ is the length of the protruding end of this pin.

Table 1 Anchoring pin loading by combination of compression and bending – section without an elastic foundation [6].

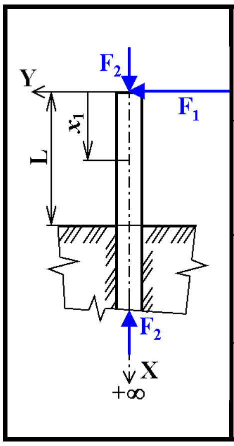

$x = x_1 \in (0;\ \mathrm{L})\,,\ N = -\mathrm{F}_2 < 0\,,\ \omega = \sqrt[4]{\frac{k_S}{4EJ_{\mathrm{ZT}}}}\,,\ \omega_{\mathrm{R}} = \sqrt{\omega^2 + \frac{\lvert N\rvert}{4EJ_{\mathrm{ZT}}}}\,,\ \omega_{\mathrm{R3}} = \sqrt{\frac{\lvert N\rvert}{EJ_{ZT}}}$
$\omega_{\mathrm{I}} = \sqrt{\omega^2 - \frac{\lvert N\rvert}{4EJ_{\mathrm{ZT}}}}\,,\ \mathrm{A}_{17} = \frac{2\mathrm{F}_1\omega^2}{\mathrm{F}_2\omega_{\mathrm{R3}}[2\omega_{\mathrm{I}}\omega_{\mathrm{R3}}\sin\omega_{\mathrm{R3}}\mathrm{L}+(\omega_{\mathrm{R3}}^2-2\omega^2)\cos\omega_{\mathrm{R3}}\mathrm{L}]}\,,\quad T = -\mathrm{F}_1$
$A_{11} = \frac{\mathrm{F}_1(2\omega_{\mathrm{R3}}[(\omega_{\mathrm{I}}+\mathrm{L}\omega^2)\omega_{\mathrm{R3}}^2-2\mathrm{L}\omega^4]\cos\omega_{\mathrm{R3}}\mathrm{L}+[(4\mathrm{L}\omega_{\mathrm{I}}+2)\omega^2\omega_{\mathrm{R3}}^2+4\omega^4-\omega_{\mathrm{R3}}^4]\sin\omega_{\mathrm{R3}}\mathrm{L})}{2\mathrm{F}_2\omega^2\omega_{\mathrm{R3}}[(2\omega^2-\omega_{\mathrm{R3}}^2)\cos\omega_{\mathrm{R3}}\mathrm{L}-2\omega_{\mathrm{I}}\omega_{\mathrm{R3}}\sin\omega_{\mathrm{R3}}\mathrm{L}]}$
$v = \mathrm{A}_{11} + \mathrm{A}_{17}\sin\omega_{\mathrm{R3}}x - \frac{\mathrm{F}_1 x}{\mathrm{F}_2}\,,\ \frac{dv}{dx} = \mathrm{A}_{17}\omega_{\mathrm{R3}}\cos\omega_{\mathrm{R3}}\,x - \frac{\mathrm{F}_1}{\mathrm{F}_2}\,,\ M_o = \mathrm{A}_{17}\mathrm{F}_2\sin\omega_{\mathrm{R3}}x$

Table 2 Anchoring pin loading by combination of compression and bending – section with an elastic foundation.

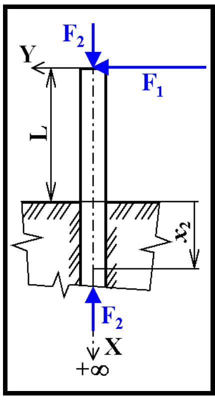

$x = x_2 \in (0;\ \infty)\,,\ -2\sqrt{k_S EJ_{\mathrm{ZT}}} < N < 0\,,\ N = -\mathrm{F}_2\,,\ \omega = \sqrt[4]{\frac{k_S}{4EJ_{\mathrm{ZT}}}}\,,\ \omega_{\mathrm{R}} = \sqrt{\omega^2 + \frac{\lvert N\rvert}{4EJ_{\mathrm{ZT}}}}$
$\omega_{\mathrm{I}} = \sqrt{\omega^2 - \frac{\lvert N\rvert}{4EJ_{\mathrm{ZT}}}}\,,\ \omega_{\mathrm{R3}} = \sqrt{\frac{\lvert N\rvert}{EJ_{ZT}}}\,,\ A_3 = \frac{\mathrm{F}_1\omega_{\mathrm{R3}}[(2\omega^2-\omega_{\mathrm{R3}}^2)\sin\omega_{\mathrm{R3}}\mathrm{L}+2\omega_{\mathrm{I}}\omega_{\mathrm{R3}}\cos\omega_{\mathrm{R3}}\mathrm{L}]}{2\mathrm{F}_2\omega^2[(2\omega^2-\omega_{\mathrm{R3}}^2)\cos\omega_{\mathrm{R3}}\mathrm{L}-2\omega_{\mathrm{I}}\omega_{\mathrm{R3}}\sin\omega_{\mathrm{R3}}\mathrm{L}]}$
$\mathrm{A}_4 = \frac{\mathrm{F}_1\omega_{\mathrm{R3}}[\omega_{\mathrm{R3}}^3\cos\omega_{\mathrm{R3}}\mathrm{L}-2\omega_{\mathrm{I}}(2\omega^2-\omega_{\mathrm{R3}}^2)\sin\omega_{\mathrm{R3}}\mathrm{L}]}{4\mathrm{F}_2\omega^2\omega_{\mathrm{R}}[2\omega_{\mathrm{I}}\omega_{\mathrm{R3}}\sin\omega_{\mathrm{R3}}\mathrm{L}+(\omega_{\mathrm{R3}}^2-2\omega^2)\cos\omega_{\mathrm{R3}}\mathrm{L}]}\,,\quad v = e^{-\omega_{\mathrm{I}}x}(\mathrm{A}_3\cos\omega_{\mathrm{R}}\,x + \mathrm{A}_4\sin\omega_{\mathrm{R}}\,x)$
$M_o = -EJ_{\mathrm{ZT}}\frac{d^2v}{dx^2}\,,\ T = N\frac{dv}{dx} - EJ_{\mathrm{ZT}}\frac{d^3v}{dx^3}$

The positive horizontal deflection v is in the direction of the coordinate axis Y.

In Table 1 and 2, there are the integration constants A_3, A_4, A_{11} and A_{17} /m/, the quadratic moment of the transversal area of this pin cross-section $J_{ZT} = (\pi D_S^4)/64$ /m4/, the modulus of elasticity of this pin material E /Pa/ and constants ω, ω_R, ω_I and ω_{R3} /m-1/. The relationships of Tab. 1 and 2 are valid for the combined stress of pressure and bending. The value of the normal pressure force then lies within the interval $-2\sqrt{k_S EJ_{ZT}} < N < 0$, which suits common practice, see references [5,13,14].

The relationships listed in Tab. 1 and 2 are therefore the solution of the two linear differential equations of the 4th order $\frac{d^4v}{dx^4} + \frac{N}{EJ_{ZT}}\frac{d^2v}{dx^2} = 0$ for $x = x_1 \in (0;\ \mathrm{L})$ and $\frac{d^4v}{dx^4} + \frac{N}{EJ_{ZT}}\frac{d^2v}{dx^2} + k_S v = 0$ for $x = x_2 \in (0;\ \infty)$. When working out the solutions the four zero integration constants (in Tab. 1 and 2, they are already used to simplify relations, i.e. not directly presented) and also the four non-zero integration constants A_3, A_4, A_{11} and A_{17}. All integration constants were determined from the following boundary conditions

$$M_o(x_1 = 0) = 0\,, \qquad T(x_1 = 0) = -\mathrm{F}_1\,, \tag{1}$$

$$\left.\begin{aligned} v(x_1 = \mathrm{L}) = v(x_2 = 0), &\qquad \frac{dv}{dx}(x_1 = \mathrm{L}) = \frac{dv}{dx}(x_2 = 0), \\ M_o(x_1 = \mathrm{L}) = M_o(x_2 = 0), &\qquad T(x_1 = \mathrm{L}) = T(x_2 = 0), \end{aligned}\right\} \tag{2}$$

$$v(x_2 \to \infty) = 0\,, \qquad v'(x_2 \to \infty) = 0. \tag{3}$$

For more information, see reference [5,13,14].

2.2 Loading by combination of tension and bending

Similarly, according to the literature [5,13–15], the general relations for the combined tension and bending can be derived. This is a solution of two differential equations of the 4th order $\frac{d^4v}{dx^4} - \frac{N}{EJ_{ZT}}\frac{d^2v}{dx^2} = 0$ for $x = x_1 \in (0;\ \mathrm{L})$ and $\frac{d^4v}{dx^4} - \frac{N}{EJ_{ZT}}\frac{d^2v}{dx^2} + k_S v = 0$ for $x = x_2 \in (0;\ \infty)$, where the boundary conditions are defined by relationships (1) to (3). The normal tensile force values are within the interval $2\sqrt{k_S EJ_{ZT}} > N > 0$, see Tab. 3 and 4. Like the above, A_3, A_4, A_{12} and A_{14}. /m/ are integration constants.

Table 3 Anchoring pin loading by combination of tension and bending – section without an elastic foundation

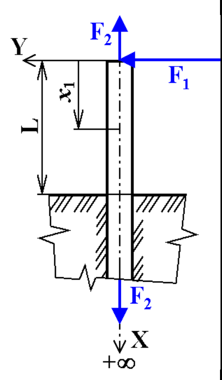	$x = x_1 \in (0;\ \mathrm{L})$, $N = \mathrm{F}_2 > 0$, $\omega = \sqrt[4]{\frac{k_S}{4EJ_{ZT}}}$, $\omega_\mathrm{R} = \sqrt{\omega^2 + \frac{\lvert N\rvert}{4EJ_{ZT}}}$, $\omega_{\mathrm{R3}} = \sqrt{\frac{N}{EJ_{ZT}}}$
	$A_{12} = \frac{\mathrm{F}_1\left(2\omega_{\mathrm{R3}}\left[(\omega_\mathrm{R}+\mathrm{L}\omega^2)\omega_{\mathrm{R3}}^2+2\mathrm{L}\omega^4\right]\cosh\omega_{\mathrm{R3}}\mathrm{L}+\left[\omega_{\mathrm{R3}}^4+(4\mathrm{L}\omega_\mathrm{R}+2)\omega^2\omega_{\mathrm{R3}}^2-4\omega^4\right]\sinh\omega_{\mathrm{R3}}\mathrm{L}\right)}{2\mathrm{F}_2\omega^2\omega_{\mathrm{R3}}\left[(2\omega^2+\omega_{\mathrm{R3}}^2)\cosh\omega_{\mathrm{R3}}\mathrm{L}+2\omega_\mathrm{R}\omega_{\mathrm{R3}}\sinh\omega_{\mathrm{R3}}\mathrm{L}\right]}$
	$\mathrm{A}_{14} = \frac{2\mathrm{F}_1\omega^2}{\mathrm{F}_2\omega_{\mathrm{R3}}\left[2\omega_\mathrm{R}\omega_{\mathrm{R3}}\sinh\omega_{\mathrm{R3}}\mathrm{L}+(\omega_{\mathrm{R3}}^2+2\omega^2)\cosh\omega_{\mathrm{R3}}\mathrm{L}\right]}$, $v = \mathrm{A}_{12} + \mathrm{A}_{14}\sinh\omega_{\mathrm{R3}}x - \frac{\mathrm{F}_1 x}{\mathrm{F}_2}$
	$\frac{dv}{dx} = \mathrm{A}_{14}\omega_{\mathrm{R3}}\cos\omega_{\mathrm{R3}}x - \frac{\mathrm{F}_1}{\mathrm{F}_2}$, $M_o = -\mathrm{A}_{14}\mathrm{F}_2\sinh\omega_{\mathrm{R3}}x$, $T = -\mathrm{F}_1$

Table 4 Anchoring pin loading by combination of tension and bending – section with an elastic foundation [6]

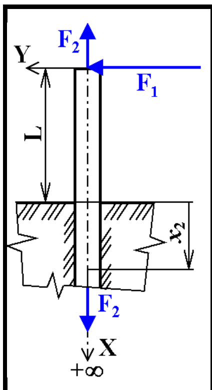	$x = x_2 \in (0;\ \infty)$, $2\sqrt{k_S EJ_{ZT}} > N > 0$, $N = \mathrm{F}_2$, $\omega = \sqrt[4]{\frac{k_S}{4EJ_{ZT}}}$, $\omega_\mathrm{R} = \sqrt{\omega^2 + \frac{\lvert N\rvert}{4EJ_{ZT}}}$
	$\omega_\mathrm{I} = \sqrt{\omega^2 - \frac{\lvert N\rvert}{4EJ_{ZT}}}$, $\omega_{\mathrm{R3}} = \sqrt{\frac{N}{EJ_{ZT}}}$, $A_3 = \frac{\mathrm{F}_1\omega_{\mathrm{R3}}\left[(2\omega^2+\omega_{\mathrm{R3}}^2)\sinh\omega_{\mathrm{R3}}\mathrm{L}+2\omega_\mathrm{R}\omega_{\mathrm{R3}}\cosh\omega_{\mathrm{R3}}\mathrm{L}\right]}{2\mathrm{F}_2\omega^2\left[2\omega_\mathrm{R}\omega_{\mathrm{R3}}\sinh\omega_{\mathrm{R3}}\mathrm{L}+(2\omega^2+\omega_{\mathrm{R3}}^2)\cosh\omega_{\mathrm{R3}}\mathrm{L}\right]}$
	$\mathrm{A}_4 = \frac{\mathrm{F}_1\omega_{\mathrm{R3}}\left[\omega_{\mathrm{R3}}^3\cosh\omega_{\mathrm{R3}}\mathrm{L}-2\omega_\mathrm{R}(2\omega^2-\omega_{\mathrm{R3}}^2)\sinh\omega_{\mathrm{R3}}\mathrm{L}\right]}{4\mathrm{F}_2\omega^2\omega_\mathrm{I}\left[2\omega_\mathrm{R}\omega_{\mathrm{R3}}\sinh\omega_{\mathrm{R3}}\mathrm{L}+(2\omega^2+\omega_{\mathrm{R3}}^2)\cosh\omega_{\mathrm{R3}}\mathrm{L}\right]}$, $v = e^{-\omega_\mathrm{R}x}(\mathrm{A}_3\cos\omega_\mathrm{I}x + \mathrm{A}_4\sin\omega_\mathrm{I}x)$
	$M_o = -EJ_{\mathrm{ZT}}\frac{d^2v}{dx^2}$, $T = N\frac{dv}{dx} - EJ_{\mathrm{ZT}}\frac{d^3v}{dx^3}$

When comparing images from Tab. 1, 2 and Tab. 3, 4, there is external force F_2 clearly acting in the opposite direction, which causes a tensional load (for normal force $N > 0$) and a compressive load (for $N < 0$).

2.3 Bending stiffness of pins

For maximum deflection $v_{\mathrm{MAX}_{N<0}}$ /m/ (at the end of a beam in points $x_1 = 0$ m) it is applied for the compression + bending loadings (i.e. situation when $N < 0$), as in Tab. 1.

$$v_{\mathrm{MAX}_{N<0}} = v(x_1 = 0) = \mathrm{A}_{11} \qquad (4)$$

Similarly, for maximum deflection $v_{\text{MAX}_{N>0}}$ /m/ (at the end of a beam in points $x_1 = 0$ m) for the tension + bending loadings (i.e. situation when $N > 0$), as in Tab. 3

Then you can determine the bending stiffness of pin k_{bend} /Nm^{-1}/, i.e. the equivalent nonlinear spring constant replacing the pin activity on the rails sections) $k_{\text{bend}} = \frac{\text{F}_1}{v_{\text{MAX}_{N<0}}}$ or $k_{\text{bend}} = \frac{\text{F}_1}{v_{\text{MAX}_{N>0}}}$, see Tab. 5.

Table 5 Relations for the bending stiffness of the pin for cases combining bending and tension/compression

	Bending stiffness of pins k_{bend}
Compression $N < 0$	$\dfrac{2\text{F}\omega^2\omega_{\text{R3}}[(2\omega^2 - \omega_{\text{R3}}^2)\cos\omega_{\text{R3}}\text{L} - 2\omega_{\text{I}}\omega_{\text{R3}}\sin\omega_{\text{R3}}\text{L}]\sin\alpha}{2\omega_{\text{R3}}[(\omega_{\text{I}} + \text{L}\omega^2)\omega_{\text{R3}}^2 - 2\text{L}\omega^4]\cos\omega_{\text{R3}}\text{L} + [(4\text{L}\omega_{\text{I}} + 2)\omega^2\omega_{\text{R3}}^2 + 4\omega^4 - \omega_{\text{R3}}^4]\sin\omega_{\text{R3}}\text{L}}$
Tension $N > 0$	$\dfrac{2\text{F}\omega^2\omega_{\text{R3}}[2\omega_{\text{R}}\omega_{\text{R3}}\sinh\omega_{\text{R3}}\text{L} + (2\omega^2 + \omega_{\text{R3}}^2)\cosh\omega_{\text{R3}}\text{L}]}{2\omega_{\text{R3}}[(\omega_{\text{R}} + \text{L}\omega^2)\omega_{\text{R3}}^2 + 2\text{L}\omega^4]\cosh\omega_{\text{R3}}\text{L} + [\omega_{\text{R3}}^4 + (4\text{L}\omega_{\text{R}} + 2)\omega^2\omega_{\text{R3}}^2 - 4\omega^4]\sinh\omega_{\text{R3}}\text{L}}$

In our cases, and from the above stated, it is clear that the bending stiffness of a beam is nonlinear but nearly linear and also dependent on external force F, angle α, on the geometry, on the material properties of pins and on the material properties of the elastic foundation in the footwall.

A deeper analysis and application for bending stiffness are explained in the 2$^{\text{nd}}$ part (follow-up) of this article, see [10]. Bending stiffness is suitable for the substitution of the pins using springs, which is advantageous for numerical solutions using FEM.

3 Load on rails and sections

For a more precise analysis of the mining train dynamic behaviour, and the sections (rails) and pins, there is usually not enough information and there is not even much willingness in mining companies to deal with this issue. This is mainly due to the low volume of mine train production, often targeted only for a single location with a specific purpose and also short-term use in one part of a mine (i.e. the entire transport system in mines often changes and moves with regard to the current needs of mining). However, the following procedure may be considered sufficient.

The dynamic load is related to extreme situations, i.e. related to sudden braking at the maximum operating speed of a mining train (the so-called hard stop).

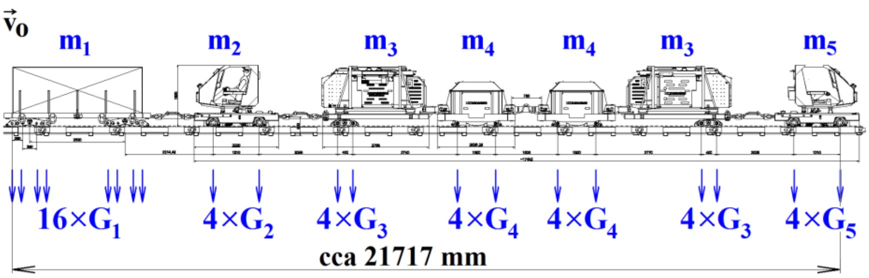

Fig. 5 Mass and gravitational force distribution acting in the rail of the mining train (horizontal movement, the vehicle consists of seven parts with partial weights m_1 to m_5)

The basic preconditions for the solution can be explained as follows. A train unit (i.e. train consisting of several trucks) is considered to be a moving system of mutually linked mass points (i.e. the common concept of dynamics) with a total weight of

$m_{total} = m_3 + m_4 + \sum_{i=1}^{5} m_i$ /kg/, where m_i /kg/ are the weights of individual trucks in this train (a part with some cargo, a part with a driver, a part with an engine, 2 braking sections, 2 propellers, and a part without a driver), see Fig. 5.

For the resulting gravitational force of a train then applies $G_{total} = m_{total} g$ /N/, where g /ms^{-2}/ is acceleration due to gravity. As shown in Fig. 5, the partial gravitational forces $G_i = m_i g / n_{wheel_i}$ /N/ can be determined, where n_{wheel_i} /1/ is the number of wheels in contact with the rails on a relevant section (truck) of this train (i.e. $n_{wheel_1} = 16$, $n_{wheel_{2,3,4,5}} = 4$). Hence, a simplistic but acceptable prerequisite is the uniform distribution of load forces G_i at the point of contact with the rail under ith truck.

It is assumed that there is equally slowed movement of a train during braking, with knowledge of initial maximum train speed v_0 /ms^{-1}/ and the length of breaking distance $s_{stop_{HORIZ}}$ /m/ at a horizontal travel (i.e. when the angle α = 0 deg, see Fig. 5). For the horizontal travel of the train it is therefore possible to derive the relationship for deceleration $a_{HORIZ} = -v_0^2/(2\ s_{stop_{HORIZ}})$ /ms^{-2}/, the time of stopping $t_{stop_{HORIZ}} = 2\ s_{stop_{HORIZ}}/v_0$ /s/ and the size of the total dynamic forces $F_{total_{HORIZ}} = \gamma_F m_{total} |a_{HORIZ}|$ /N/, where γ_F /1/ is the dynamic coefficient respecting the potential increase in dynamic forces due to real inequalities and the asymmetry of the section system, the irregularity of propulsion, the distribution of loads, and contact of the wheels and rails of the section.

The next derivation of the dynamic behaviour when the train is braking is based on the transferability of the dynamic behaviour in a horizontal line on an inclined line. For the resulting braking force $F_{total_{BREAK}}$ /N/ then there are the sufficiently enough valid relations entered in Tab. 6.

Table 6 Generalized relations for the braking force. [6]

	The total braking dynamic force from the train
The decline of the train 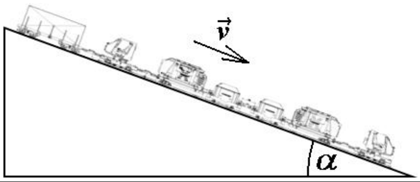	$F_{total_{BREAK}} = F_{total_{HORIZ}} + \gamma_F G \sin\alpha = \gamma_F m_{total}[v_0^2/(2\ s_{stop,_{HORIZ}}) + g \sin\alpha]$
Horizontal travel 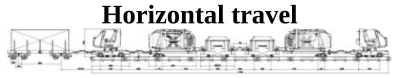	$F_{total_{BREAK}} = F_{total_{HORIZ}} = \gamma_F m_{total}\ v_0^2/(2\ s_{stop_{HORIZ}})$
The ascend of the train 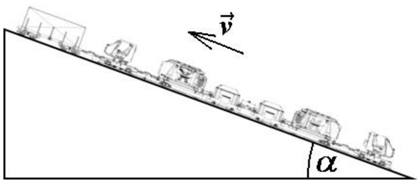	$F_{total_{BREAK}} = F_{total_{HORIZ}} - \gamma_F G \sin\alpha = \gamma_F m_{total}[v_0^2/(2\ s_{stop_{HORIZ}}) - g \sin\alpha]$

From the results of Tab. 6, it is clear that the maximum braking forces transferred to the sections occur, when driving on decline gradients (downward travel of a train after dip, i.e. α > 0 deg) and it is on a decline gradient (extreme load forces) and horizontal travel is aimed to work more.

Dynamic braking pressure is transmitted through the braking trucks into sections of two braking places using forces $F_{dyn} = \gamma_{rail} F_{total_{BREAK}}/4$ /N/ and tilting moment (tilting couple) $M_{dyn} = F_{dyn} r_{dyn}$ /Nm/, where γ_{rail} /1/ is the loss coefficient, which respects the possible dynamic losses (damping, friction between a footwall and sections, dynamic effects do not act only in four places of rails, etc.) and r_{dyn} /m/ is the arm of the tilting moment, see Fig. 6. It is obvious that $\gamma_{rail} \leq 1$ and also that r_{dyn} are related to the position of the centre of gravity for the entire system, and its distance from the rail section centreline.

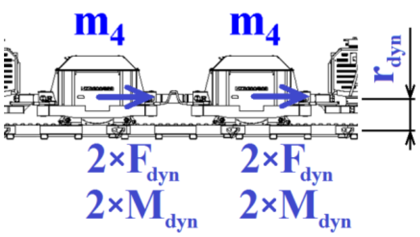

Fig. 6 Transmission of dynamic effects to sections when a train is braking using two braking elements

In accordance with the theory of beams on the elastic Winkler foundation, see [5,13–16], you can replace the rails and the sections on the footwall with an equivalent stiffness $k_{sect} = K_{sect}b_{sect}$ /Pa/, see Fig. 7, where K_{sect} /Nm^{-3}/ is the module of a section subsoil and b_{sect} /m/ is the width of the section rails.

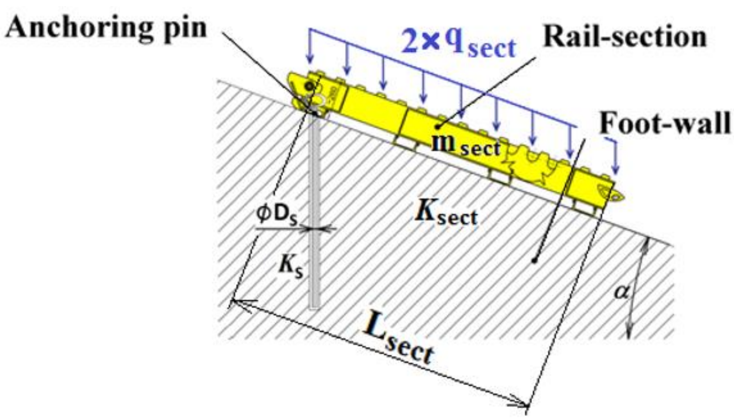

Fig. 7 Placement of sections on a footwall and the static load of sections from its own weight.

Section load from the own weight of the section m_{sect} /kg/, see Fig. 7, can be defined using equal continuous load $q_{sect} = m_{sect}g/(2L_{sect})$ /Nm^{-1}/ which acts on both rails along the whole length of the section L_{sect} /m/. It is clear that q_{sect} acts independently on each rail, in the vertical direction (i.e. in the direction of gravitational acceleration).

4 Applying the Finite Element Method

It is assumed that the train is in the middle of a designed rail section with a selected length $11 \times 2L_{sect}$, see Fig. 8. All rail loads have already been explained in the preceding chapters.

According to the considerations stated in the previous chapters, it is possible to create a plane beam model for a sufficiently long section of rails with 11 anchoring pins, see Fig. 2, 8 and 9 (ANSYS software, FEM). It is assumed that all the static and dynamic loads are captured by 11 pins on the right side of the section, 11 pins on the left side of the section, the rail sections, and the placement of a footwall (elastic foundation).

For practical reasons the rail is equipped with spring fixings on both ends (an attempt to include the effect of the real rail end point using axial stiffness k_{end} /Nm-1/), see Fig. 8.

The pins can also be simply replaced using springs located in the axial direction of the rails (rigidity k_{bend}, see Chapter 2). The train is located in the middle of a track section ,with the length $11 \times 2\mathrm{L}_{\mathrm{sect}}$, see Fig. 8.

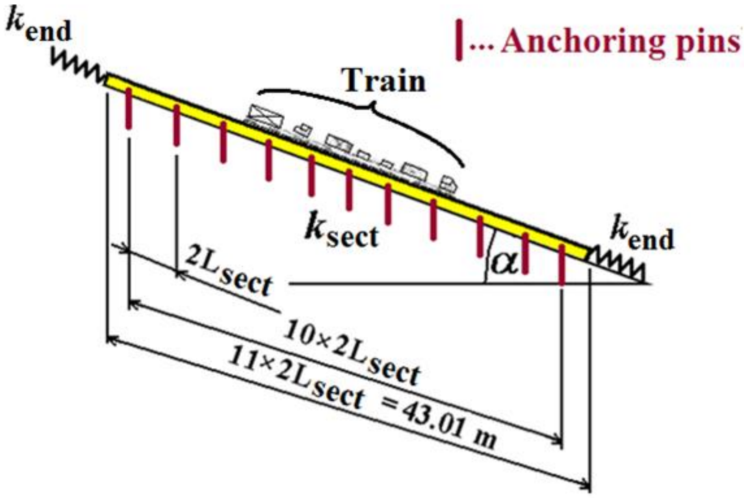

Fig. 8 Designed section of a rail banked under general angle α

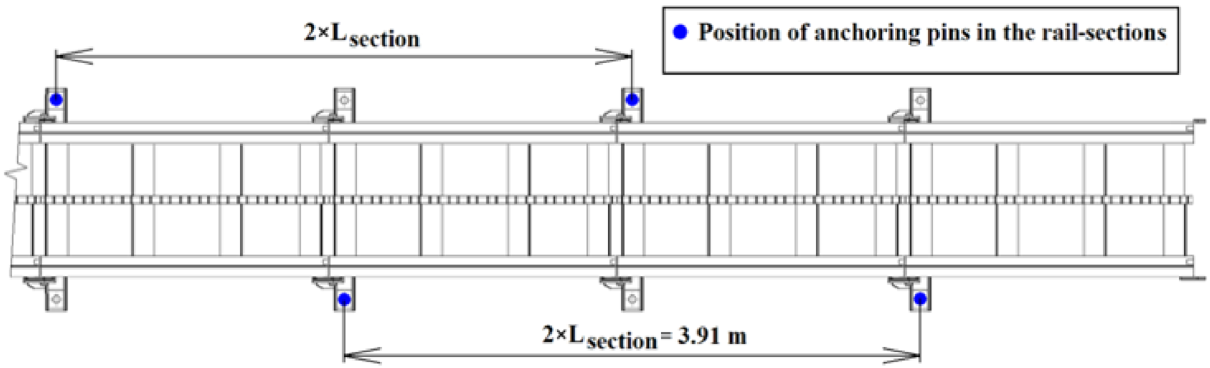

Fig. 9 Top view on the sections system placed on a footwall [6]

The spacing of anchoring pins, resulting from the assignment, is explained in Fig. 8 and 9.

The examples of calculation models for solutions using FEM are shown e.g. in Fig. 10 (angle of slope inclination $\alpha = 0$ to 25 deg).

In the ANSYS program the plane beam elements "Beam54" were used together with spring elements "Combin14".

5 The processing of results

Calculations using FEM are carried out according to the theory of the 1st order (i.e. the effect of normal forces is taken into account simply only in stiffness k_{end} and k_{bend}, see Tab. 5, which is acceptable and with little error, in particular for calculations of transverse and longitudinal deflections). FEM is used to solve deflections, slope (rotations), bending moments, shearing forces and normal forces in the rails of the sections, and also for the force action/reaction F_1 and F_2.

The next step is the processing of the FEM results for the resulting stress on the anchoring pins. This is dealt with separately using an analytical approach according to the more accurate theory of the 2nd order. The ANSYS program does not allow a direct solution according to the theory of the 2nd order. In other words, the ANSYS program will help to determine forces F_1 and F_2 (the forces acting on an anchoring pin, finds a maximum value etc.) and according to the relations of Tab. 1, 2 and 3, 4 deflection dependencies, slope, bending moments, shearing forces and normal forces can be determined in the anchoring pins.

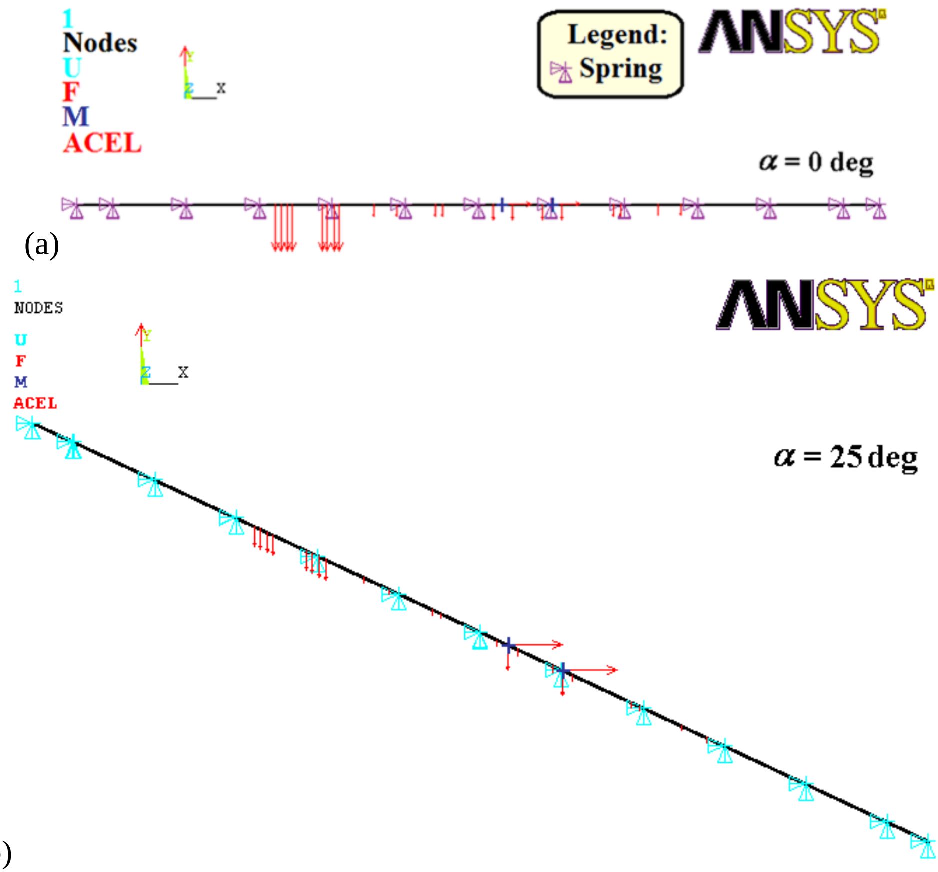

Fig. 10 Examples of beam mesh of finite elements, boundary conditions, and loads (FEM, software ANSYS), see [6], (a) Horizontal position, (b) Decline position

Hence, our presented approach (i.e. combination of analytical approach and numerical FEM Ansys approach) should be more accurate in comparing to only simple beam FEM Ansys software approach.

From the known values of the bending moments and normal forces the extreme stresses $\sigma_{\max,\min}$ /Pa/ can be determined for combined stress (i.e. tension/compression and bending) according to the known relations of strength and elasticity of materials, see, e.g. [7],

$$\sigma_{\max,\min} = \max \& \min\left(\frac{N}{\frac{\pi D_S^2}{4}} \pm \frac{M_O}{\frac{\pi D_S^3}{32}}\right) = \max \& \min\left[\frac{4}{\pi D_S^2}\left(N \pm \frac{8M_O}{D_S}\right)\right] \quad (6)$$

The practical results are the main topic of the second part in this article. An example of processing the results is given in Fig. 11 and 12.

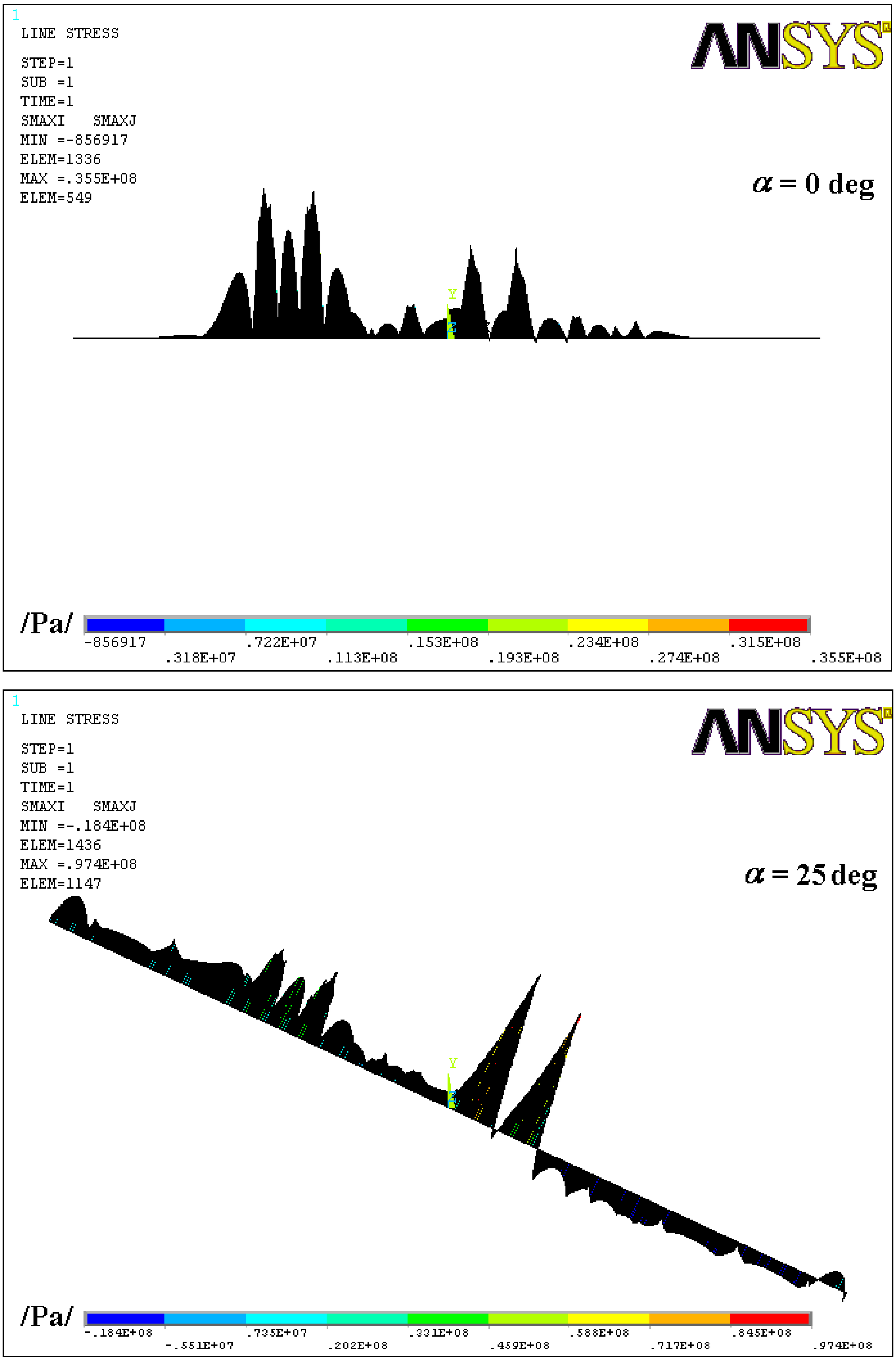

Fig. 11 Resulting maximum stress σ_{max} in a rail section for the inclination angle α = 0 deg and α = 25 deg (FEM, ANSYS software, hard stop)

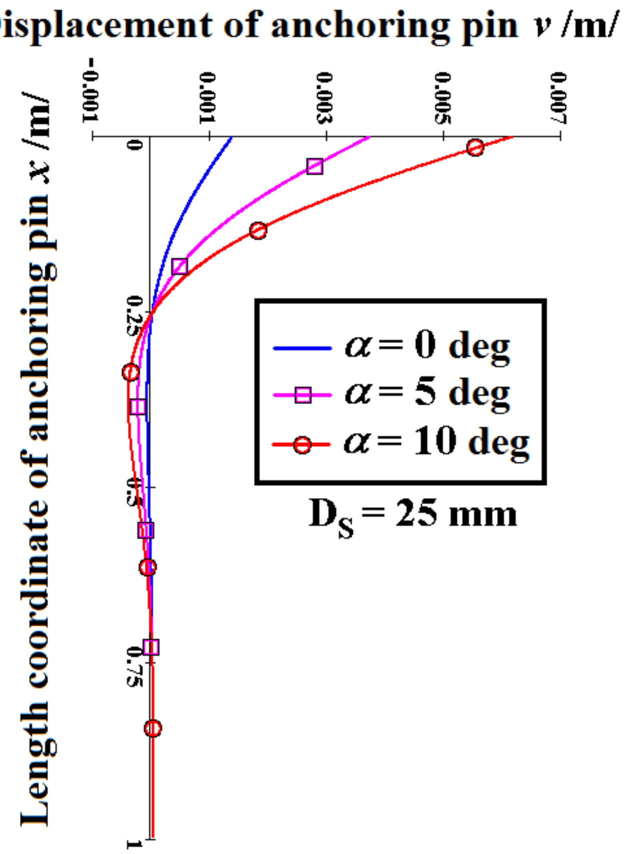

Fig. 12 Behaviour of horizontal deflections in anchoring pins according to Tab. 3, 4 and FEM for inclination angles α = 0, 5 and 10 deg [6]

6 Discussion and other possible methods of solution

The above-stated authors' procedure for dealing with complex tasks of the mechanical interaction between a mining-rack railway track, and sections with rails and its anchoring pins, is practical and sufficient. However, for a deeper examination and further development there are several possible improvements.

A further innovative approach is also the use of probabilistic methods. The team of authors has extensive experience with the application of the Simulation-Based Reliability Assessment (SBRA) Method, which uses the direct Monte Carlo method in biomechanics, mining, civil and mechanical engineering. However, probabilistic method can be also used in the rack-railway tracks. Its advantage is that the inputs and outputs are given by bounded histograms, which respect the real variability of physical quantities (i.e. the geometry of structure, the placement of the structure on the mining amended the placement on footwall damaged by mining activities, material behaviour, dynamics and static load, etc.). The disadvantage is the multiple repetition of calculations for predefined random inputs (simulation method), which places greater demands on computing and is a time-consuming solution. For a closer look, see for example the solution of other types of jobs in references [21–24] and in the example of Fig. 13. The application of the SBRA Method, as the current trend of a stochastic mechanics, associated with the probability assessment on reliability, will be the subject of the future solution for these jobs, see [25–29].

Research of residual stresses in rack-railway track could be solved too, see [6,30,31].

One of the possible solutions is also to implement repeated measurements on a real mining track. But there is no room for such measurements, for the technical and economic reasons listed at the beginning of Chapter 3 (i.e. the low volume of mining trains production often designed only for a single location, for a short-term use in some current part of a mine; complex, expensive and the time-consuming preparation of measurement associated with potential downtimes). Yet it is clear that this experiment is a suitable and desirable contribution to the solution of such complex issues. For example, see [32–35].

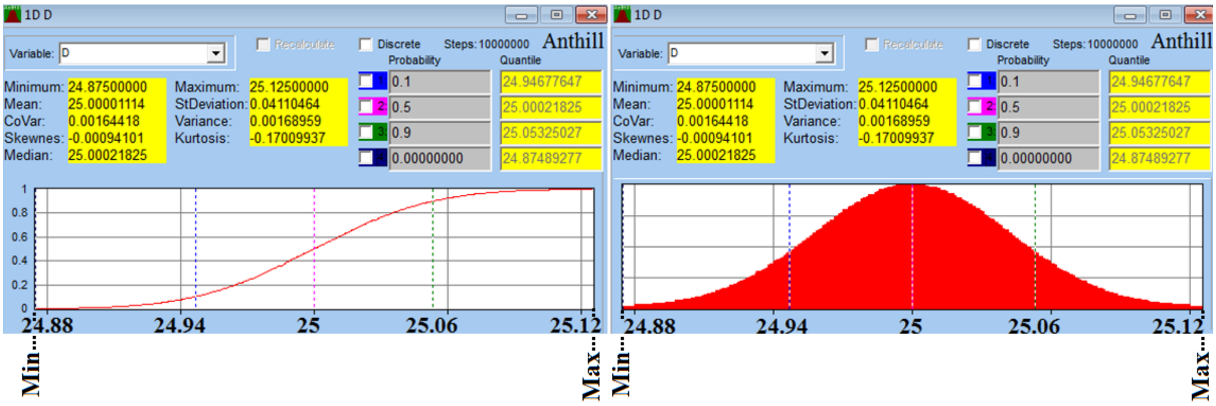

Fig. 13 Distribution function and the histogram of the parameter $D_S = 25 \pm 5‰$ mm (SBRA Method Anthill, software, the result of 10^7 Monte Carlo pseudorandom simulations)

It is also possible to offer the solution of applying load in the curves and switches of the rack-railway tracks, which is a more complex task.

It is also possible to use the shell or space (3D) model using the volume elements of the Finite Element Method, see [27]. This will bring a more complex and challenging solution to the demanding tasks of the mechanical contact between the sections and footwalls, and the sections and pins. However, the elegance and speed of calculating the presented analytical-numerical model will disappear.

The presented Bernouli-beam approach does not consider the influence of transversal factor. Therefore, in a further study, the Timoshenko-beam can be considered or other types of elastic foundations can be applied, for example, see [36–39].

CONCLUSION

This article presents an original and relatively simple method of determining the deformation and tensions in the pins and rails of the sections systems placed on footwalls (analytical-numerical model). The placement of the rack-railway track sections and anchoring pins is replaced by the popular linear bilateral Winkler model of elastic foundation.

The whole system bears the static load from the own weight of the rack-railway structure design, and also the dynamics from the weight of the mining train, and the braking force and braking moment caused by breaking trucks (a hard stop - an unfavourable situation load in emergency situations).

The new part here is the combination of analytical approaches according to the theory of the 2nd order beams placed on the elastic foundation (the issue of anchoring pins) and numerical approaches (FEM, ANSYS software) according to the lower theory of the 1st order (the issue of rails) which are mutually interconnected.

The application of elastic foundation is very suitable for all mine placements on footwalls or in footwalls.

The theory is clarified and the overall analysis of the load, and of the peripheral conditions, and dynamics of loading is explained. The same is true also for the calculation of stress and deformation for the entire complex system.

From the perspective of the strength and elasticity of materials the entire system is loaded predominantly by the combination of tension/compression and bending.

This procedure is possible, after its modification, to use for horizontal lifting mining systems, see for example Fig. 14a, or for design calculations of similar structures outside the field of mining engineering, see for example Fig. 14b.

Fig. 14 Suspended mining locomotive and Singapore Sentosa monorail

Non-traditional interconnection of the analytical approach and FEM brings new and fresh insights into the often neglected and not very often published issues.

ACKNOWLEDGEMENTS

This article was supported by a Czech project SP2024/037, SP2024/01 and by projects CZ.02.1.01/0.0/17_049/0008407 and CZ.02.1.01/0.0/0.0/17_049/0008441 within the Operational Programme Research, Development, and Education financed by the European Union and from the state budget of the Czech Republic.

REFERENCES

[1] Frydrýšek, K., Fries, J. "Stress Calculations in the Rails and Anchor Pins of Sections DS=25 mm depended on incline angle - Calculation report (Výpočty napětí v kolejnici sekce a svorníku sekce DS=25 mm v závislosti na úhlu sklonu dráhy – Výpočtová zpráva) ", Department of Mechanics of Materials, Faculty of Mechanical engineering, VŠB – Technical University of Ostrava, Ostrava, Czech Republic, pp. 1 – 35, **2010**. Written in Czech language.

[2] Halama, R., Fajkoš, R., Matušek, P., Bábková, P., Fojtík, F., Václavek, L. "Contact Defects Initiation in Railroad Wheels – Experience, Experiments and Modelling", Wear 271, pp.174 – 185, **2011**.

[3] Hay, W.W. "Railway Engineering, Encyclopedia of Physical Science and Technology" (Third Edition); University of Illinois: Illinois, USA, pp. 807 – 844, **2003**. DOI:10.1016/B0-12-227410-5/00650-5

[4] Pascal, J.P. "Oscillations and Chaotic Behaviour of Unstable Railway Wagons over Large Distances", Chaos, Solitons & Fractals, 5 (9), pp. 1725 – 1753, **1995**. DOI: 10.1016/0960-0779(94)00173-N

[5] Frydrýšek, K. "Beams and Frames on Elastic Foundation 1 (Nosníky a rámy na pružném podkladu 1)"; Faculty of Mechanical Engineering, VŠB - Technical University of

Ostrava, Ostrava, Czech Republic, pp. 463, **2006**. ISBN 80-248-1244-4. Written in Czech language.

[6] Frydrýšek, K., Fries, J. "Stresses and Deflections of Rail and Anchor Pin in the Dependence on the Slope Angle of the Railway in Mines", International Scientic Conference Mechanical Structures and Foundation Engineering MSFE 2010, Ostrava, pp. 1 – 6, **2010**.

[7] Frydrýšek, K. "Basic Strength and Elasticity of Materials"; Faculty of Mechanical Engineering, VŠB – Technical University of Ostrava, Ostrava, Czech Republic, pp. 1 – 264, **2016**. ISBN 978-80-248-3870-0.

[8] Galishnikova, V., Gebre, T.H., Al-Sabri, S,M, Saffia-Doe, O. "Second Order Structural Theory for the Stability Analysis of Columns", Structural Mechanics of Engineering Constructions and Buildings 14 (3), pp. 192 – 197, **2018**. DOI: 10.22363/1815-5235-2018-14-3-192-197

[9] Gräbe, P. J., Clayton, C. R. "Effects of principal stress rotation on permanent deformation in rail track foundations", Journal of Geotechnical and Geoenvironmental Engineering, 135 (4), pp. 555 – 565, **2009**.

[10] Tucho, A., Indraratna, B., Ngo, T. "Stress-deformation analysis of rail substructure under moving wheel load", Transportation Geotechnics 36, 100805, **2022**. DOI: 10.1016/j.trgeo.2022.100805

[11] Tzanakakis, K. "The railway track and its long term behaviour: a handbook for a railway track of high quality", Vol. 2. Springer Science & Business Media, **2013**. ISBN: 978-3-642-36051-0

[12] Janeras, M., Jara, J., Royán, M.J et al. "Multi-technique approach to rockfall monitoring in the Montserrat massif (Catalonia, NE Spain)", Engineering geology 219, pp. 4 – 20, **2017**. DOI: 10.1016/j.enggeo.2016.12.010

[13] Frydrýšek, K., Jančo, R. et al. "Beams and Frames on Elastic Foundation 2 (Nosníky a rámy na pružném podkladu 2) ", Faculty of Mechanical Engineering, VŠB - Technical University of Ostrava, Ostrava, Czech Republic, **2008**, pp. 516. ISBN 978-80-248-1743-9. Written in Czech and English.

[14] Frydrýšek, K., Nikodým, M. et al. "Beams and Frames on Elastic Foundation 3 (Nosníky a rámy na pružném podkladu 3) ", VŠB – Technical University of Ostrava, Ostrava, Czech Republic, **2010**, pp.611. ISBN 978-80-248-2257-0. Written in Czech and English.

[15] Frydrýšek, K., Fries, J. et al. "Aplikace konstrukcí na pružném podkladu", VŠB - Technical University of Ostrava, Ostrava, Czech Republic, **2010**, pp.204. ISBN 978-80-248-2361-4. Written in Czech.

[16] Hetényi, M. "Beams on Elastic Foundation", Ann Arbor, University of Michigan Studies, USA, **1964**.

[17] Melerski, E., S. "Design Analysis of Beams, Circular Plates and Cylindrical Tanks on Elastic Foundations", London, UK: Taylor & Francis Group, **2006**. ISBN 978-0-415-38350-9.

[18] Tsudik, E. "Analysis of Beams and Frames on Elastic Foundation", USA: Trafford Publishing, **2006**. ISBN 1-4120-7950-0.

[19] Yue, F., Wu, Z., Fan, Z., Li, H. "Two Novel Vlasov Models for Bending Analysis of Finite-Length Beams Embedded in Elastic Foundations", Buildings 12 (8), 1122, **2022**. DOI: 10.3390/buildings12081122

[20] Stampka, K., Sarradj, E. "A Time-Domain Finite-Difference Method for Bending Waves on Infinite Beams on an Elastic Foundation", Acoustics 4 (4), pp. 867 – 884, **2022**. DOI: 10.3390/acoustics4040052

[21] Frydrýšek, K., Pečenka, L. "Probabilistic Evaluation of Residual Stresses for Hole-Drilling Tests", Applied Mechanics and Materials 684, pp. 400 – 406, **2014**. ISSN: 1660-9336, DOI: 10.4028/www.scientific.net/AMM.684.400

[22] Frydrýšek, K. "Probabilistic approaches applied in the solution of problems in mining and biomechanics", In Proceedings of the 17th International Conference ENGINEERING MECHANICS 2011, Svratka, Czech Republic, 9 – 12 May 2011; pp. 151 – 154, **2011**. ISBN 978-80-87012-33-8

[23] Frydrýšek, K., Marek, P. "Probabilistic solution and reliability assessment of the hard rock disintegration proces", Reliability, Risk and Safety: Theory and Applications 1-3, European Safety and Reliability Conference (ESREL 2009), Prague, Czech Republic, pp. 1443 – 1450, **2009**. ISBN: 978-0-415-55509-8

[24] Marek, P., Brozzetti, J., Guštar, M., Tikalsky P. "Probabilistic Assessment of Structures Using Monte Carlo Simulation Background, Exercises and Software", (2nd extended edition); ITAM CAS, Prague, Czech Republic, pp. 1 – 471, **2003**. ISBN 80-86246-19-1

[25] Frydrýšek, K., Čepica, D., Halo, T. "Biomechanics - Probabilistic anthropometry approach for sitting human and seat", In Proceedings of the Experimental Stress Analysis - 57th International Scientific Conference, EAN 2019, Praha, Czech Republic, pp. 90 – 96, **2019**. ISBN 978-80-214-5766-9

[26] Frydrýšek, K., Šír, M., Pleva, L., Szeliga, J., Stránský, J., Čepica, D., Kratochvíl, J., Koutecký, J., Madeja, R., Dědková, K.P., Stančeková, D. "Stochastic Strength Analyses of Screws for Femoral Neck Fractures", Appl. Sci. 12, 1015, **2022**. DOI: 10.3390/app12031015

[27] Tvrdá, K. "Foundation Plate on the Elastic Half-Space, Deterministic and Probabilistic Approach", In Proceedings of the Conference on Dynamics of Civil Engineering and Transport Structures and Wind Engineering Dyn-Wind’2017, MATEC Web of Conferences, Bratislava, Slovakia, 21–25 May 2017; Volume 107. no. 00058, **2017**.

[28] Monjardin-Quevedo, J.G., Valenzuela-Beltran, F., Reyes-Salazar, A., Leal-Graciano, J.M., Torres-Carrillo, X.G., Gaxiola-Camacho, J.R. "Probabilistic Assessment of Buildings Subjected to Multi-Level Earthquake Loading Based on the PBSD Concept", Buildings 12, 1942, **2022**. DOI: 10.3390/buildings12111942

[29] Malerová, L., Pokorný, J., Kristlová, E., Wojnarova, J. "Using of mobile flood protection on the territory of the Moldova as possible protection of the community", IOP Conf. Ser. Earth Environ. Sci. 92, 12039, **2017**. DOI: 10.1088/1755-1315/92/1/012039

[30] Orringer, O. "How Residual Stresses can Affect Rail Performance", In: Kalker, J.J., Cannon, D.F., Orringer, O. (eds) "Rail Quality and Maintenance for Modern Railway Operation", Springer, Dordrecht, **1993**. DOI: 10.1007/978-94-015-8151-6_20

[31] Kanga, C., Wenner, M., Marx, S. "Experimental investigation on the rail residual stress distribution and its influence on the bending fatigue resistance of rails", Construction and Building Materials 284, 122856, **2021**.

[32] Fedorko, G., Molnar, V., Marasova, D. et al. "Failure analysis of belt conveyor damage caused by the falling material. Part I: Experimental measurements and regression models", Engineering failure analysis 36, pp. 30 – 38, **2014**. DOI: 10.1016/j.engfailanal.2013.09.017.

[33] Famfulík, J., Miková, J., Lanská, M., Richtář, M. "A stochastic model of the logistics actions required to ensure the availability of spare parts during maintenance of railway vehicles", Proc. Inst. Mech. Eng. Part F 228, pp. 85 – 92, **2014**. DOI: 10.1177/0954409712465695

[34] Hrabovský, L. "Tension force equalizer in a rope system using a proximity sensor", Sci. J. Sil. Univ. Technol. Ser. Transp. 110, pp. 35 – 44, **2021**. DOI: 10.20858/sjsutst.2021.110.3 .

[35] Šlesar, P., Jančo, R. "Strength and Dynamic Assessment of Cage and Bearing for Railway Carriage", Strojnícky časopis – Journal of Mechanical Engineering 70 (1), pp. 127 – 134, **2020**. DOI: 10.2478/scjme-2020-0012

[36] Lecture 8: "Beam Theory in FEA- Euler-Bernoulli vs Timoshenko" - YouTube, https://www.youtube.com/watch?v=-K3sPfl6RP8

[37] Wang, C. M., K. Y. Lam, and X. Q. He. "Exact solutions for Timoshenko beams on elastic foundations using green's Functions∗", Journal of Structural Mechanics 26 (1), pp. 101 – 113, **1998**. DOI: 10.1080/08905459808945422

[38] Lolov, D., Lilkova-Markova, S. "Dynamic Stability Of An Inclined Fluid-Conveying Pipe With A One-Sided Elastic Support", Strojnícky časopis – Journal of Mechanical Engineering 74 (1), pp. 57 – 62, **2024**. DOI: 10.2478/scjme-2024-0006

[39] Lolov, D., Lilkova-Markova, S. "The Model of Interconnected Pipes in the Investigation of Dynamic Stability of Carbon Nanotubes Embedded in an Elastic Medium", Strojnícky časopis – Journal of Mechanical Engineering 73 (2), pp. 93 – 98, **2023**. DOI: 10.2478/scjme-2023-0024